processes

MDPI

Review

Non-Classical Circularly Polarized Luminescence Control of Peptide Luminophore Based on Precise Chiral Space Control

Yoshitane Imai * and Mizuki Kitamatsu *

Department of Applied Chemistry, Faculty of Science and Engineering, Kindai University, 3-4-1 Kowakae, Higashiosaka 577-8502, Japan

* Correspondence: y-imai@apch.kindai.ac.jp (Y.I.); kitamatu@apch.kindai.ac.jp (M.K.)

Abstract: Light that rotates in a circular spiral when viewed from the front is known as circularly polarized luminescence (CPL), and can be divided into two types, namely, left- and right-rotating light. To emit both left- and right-rotating CPLs, two types of optically active luminophores, namely, enantiomer *D*- and *L*-bodies, are generally required. This mini-review mainly discusses our latest study on CPL properties via the control of the pyrene ring as the luminescent unit incorporated into chiral peptides. In this study, optically active peptide–pyrene organoluminescent materials that emit CPL were synthesized by combining a peptide as a frame and two pyrene rings as a luminescent unit. By adjusting the interpyrene distance, external conditions, and absolute chiral configuration (*D*- or *L*-configuration), the chiral spatial configuration of the luminescent pyrene ring was precisely controlled. Consequently, the direction of CPL rotation from pyrenylalanine-containing peptides with the same configuration was successfully controlled.

Keywords: chiral molecule; circularly polarized luminescence (CPL); peptide; pyrene

Citation: Imai, Y.; Kitamatsu, M. Non-Classical Circularly Polarized Luminescence Control of Peptide Luminophore Based on Precise Chiral Space Control. *Processes* **2023**, *11*, 2778. https://doi.org/10.3390/pr11092778

Academic Editors: Kenji Usui, Kin-ya Tomizaki and Yonghui Li

Received: 31 July 2023
Revised: 6 September 2023
Accepted: 15 September 2023
Published: 17 September 2023

1. Introduction

Polarized light refers to light that exhibits oscillations in a particular direction, whereas circularly polarized luminescence (CPL) is used to describe light that rotates in a spiral pattern and can be categorized into left- and right-rotating light (Figure 1).

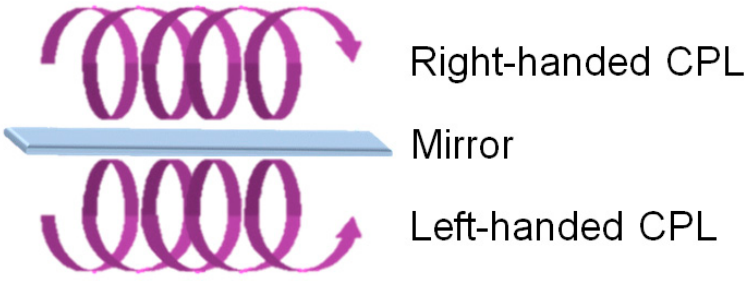

Figure 1. Mirror image of CPL.

CPL can be used in various applications, including energy-efficient three-dimensional displays, advanced security tags, and LED-based plant growth control, and new industries using this special polarized light are expected to emerge. However, because the light emitters of CPL light sources currently in use do not have CPL properties, circular polarization filters are used to convert linearly polarized light into circularly polarized light, producing left and right circularly polarized luminescence. However, in this method, the use of a circular polarization filter causes a significant reduction in light intensity. If a CPL emitter is used as the light emitter, CPL can be produced without any reduction in the light intensity, enabling a significant improvement in energy efficiency. In other words, the use

of CPL-type light emitters makes it possible to achieve a significant improvement in energy efficiency and high functionality simultaneously. The production of left- and right-handed CPLs typically necessitates the use of two distinct types of optically active luminescent materials, namely, enantiomers *D* and *L*. The generation of both left- and right-handed CPLs from an optically active luminescent material with only one chirality will reduce the material cost and production time to obtain CPLs. Moreover, it may be possible to develop luminescent materials for CPLs using natural compounds or biomolecules. The development of luminescent CPL materials using biomolecules has been reviewed by Qu's group [1].

This review describes methods for the generation and control of both left- and right-handed CPLs from an identical organoluminescent material consisting of an optically active peptide–pyrene structure. A peptide has been used as a scaffold to bind pyrene, and CPL studies that used such a structure were reported in the 1980s [2–6]. However, these studies were limited to peptide synthesis via polymerization, and the compounds used lacked a well-defined structure owing to the distribution of molecular sizes. Therefore, these compounds may not be suitable for controlling CPL. The authors expect that CPL can be more precisely controlled using solid-phase peptide synthesis to obtain peptides with well-defined structures.

Some research groups that conducted studies on the peptide-based regulation of CPLs recently reported that they succeeded in generating CPL from achiral molecules incorporated into peptide assemblies and peptide-based assemblies [7–15]. These research groups used peptides of various sizes, from dipeptides to polymeric peptides, to form peptide aggregates. A feature of these methods is that the chiral field generated by the aggregates triggers the generation of CPL from achiral molecules. In addition to these reports, Xin's group reported that CPL was generated from soft hydrogels with aggregation-induced luminescence obtained via interacting the six-core Ag(I) nanoclusters with an oligo-aspartic acid in water [16,17]. This method is characterized by the specific fluorescence detection of the amino acid Arg.

Cao's group investigated a method that does not use a peptide assembly and reported that CPL is induced by incorporating chiral dipeptides composed of aromatic amino acids into achiral supramolecules composed of tetraphenylethylene (TPE) units [18]. Their research group also reported that the interaction of an achiral supramolecular organic framework with an L-form dipeptide successfully generated the N-terminal amino acid-dependent CPL of the dipeptide [19]. Furthermore, Xing's group reported that the specific binding of a tryptophan-containing dipeptide to an acceptor, such as aromatic molecules, induces CPL from the nonemissive peptide [20]. These methods that use dipeptides as triggers for the generation of CPL will continue to receive increasing research interest in the future.

In terms of research on the application of CPL in cells, Parker's group noted that Eu (III) complexes containing ammonium salts can regulate CPL by interacting with various phosphorylated hexapeptides [21]. Because this method can detect phosphorylated amino acids, there is a possibility of the intracellular utilization of CPL. Additionally, Shi et al. reported that fluorescent TPE-modified peptide analogues facilitated the intramolecular assembly of TPE and successfully generated CPL [22]. This method is unique and can be utilized to align many fluorescent dyes on the peptide using a single peptide molecule as a template.

Apart from the above-mentioned research, Wu's group reported on CPL generated from complexes of Eu (III) with various short histidine-containing peptides [23]. Duan's group also used the complexes of cyclodextrins with pyrene-modified branched peptides, and they demonstrated the regulation of pyrene-derived CPLs depending on the cyclodextrin cavity size [24].

Although these studies differ from our concept of CPL regulation, they are significant studies on CPL regulation using peptides. The present study also demonstrates that peptide–pyrene organoluminescent materials can control CPLs as well as the intensity

of the CPLs. The manipulation of non-classical CPL properties via the precise control of the chiral space associated with the luminescent pyrene unit is discussed through a demonstration.

2. Control of Configuration-Dependent CPL Properties in Optically Active Peptide–Pyrene Organoluminescent Materials [25]

Four optically active peptide–pyrene organoluminescent materials, namely, (L)-**1**, (L)-**2**, (D)-**1**, and (D)-**2**, were newly designed by combining a peptide as a frame with a luminescent pyrene unit (Figure 2). These peptides were synthesized using the Fmoc-based solid-phase peptide synthesis method [26–28] using Fmoc-Eg6-OH, Fmoc-L-Ala(Pyr)-OH, and Fmoc-D-Ala(Pyr)-OH. All peptides used in this study have a hexethylene glycol (Eg6) unit attached to both ends of the peptides. The Eg6 unit was expected to improve the affinity of peptides for various solvents, which aided in the assessment of the peptides for the solvents described below (Section 6).

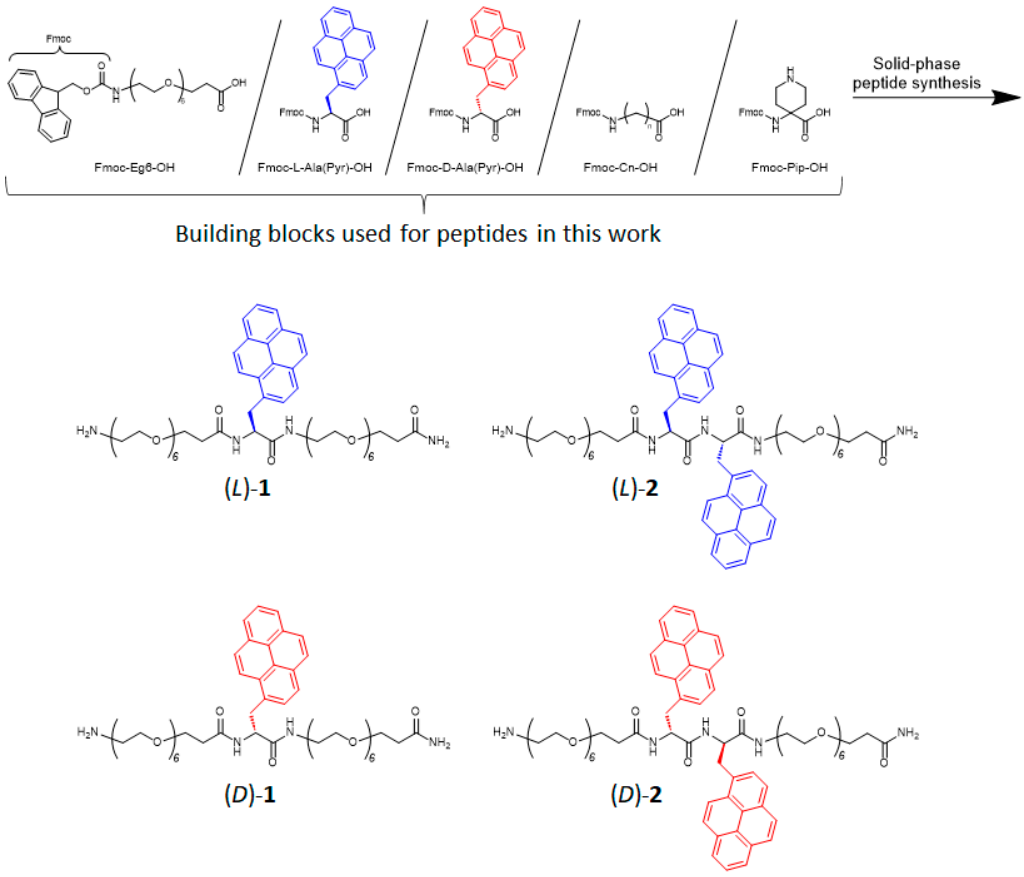

Figure 2. Scheme of the solid-phase peptide synthesis and chemical structures of chiral peptide–pyrene luminophores: (L)-**1**, (L)-**2**, (D)-**1**, and (D)-**2**.

The chiroptical properties of these four peptide luminophores were investigated in a chloroform ($CHCl_3$) solution. First, the circular dichroism (CD) spectra were determined to assess the chiral environment of the luminescent pyrene units in their ground state (Figure 3).

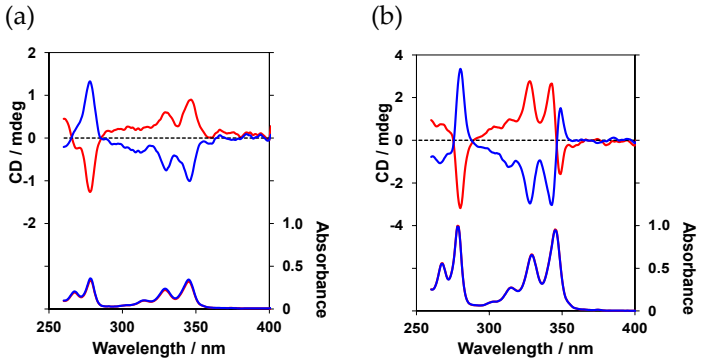

Figure 3. CD (top) and absorption (bottom) spectra of (**a**) (L)-**1** (blue lines) and (D)-**1** (red lines), and (**b**) (L)-**2** (blue lines) and (D)-**2** (red lines) in $CHCl_3$ solutions.

The absorption wavelengths of (L)-**1** and (L)-**2** were not significantly different. However, a large distinction emerged in the CD spectrum, where (L)-**1** exhibited a negative (–) Cotton effect, whereas (L)-**2** exhibited a positive (+) Cotton effect. The photoluminescence (PL) and CPL spectra were determined in a $CHCl_3$ solution (Figure 4).

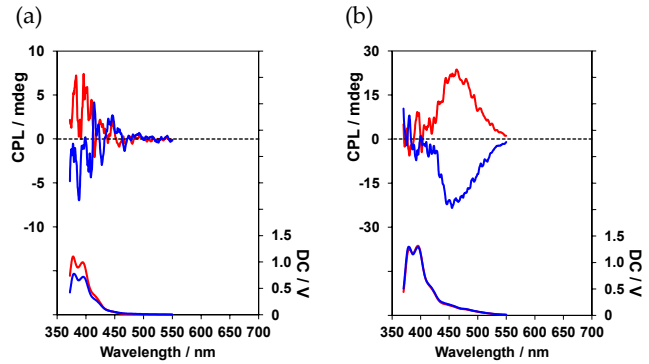

Figure 4. CPL (top) and PL (bottom) spectra of (**a**) (L)-**1** (blue lines) and (D)-**1** (red lines), and (**b**) (L)-**2** (blue lines) and (D)-**2** (red lines) in $CHCl_3$ solutions.

The CPL spectra of (L)-**1** and (L)-**2** were significantly different. (L)-**1**, with one pyrene unit, emitted weak monomeric CPL at a maximum luminescence wavelength (λ_{em}) of approximately 378 nm. In contrast, (L)-**2,** with two pyrene units, emitted strong excimer CPL at λ_{em} of approximately 455 nm. The sign of the CPL profiles between (L)-**2** and (D)-2 were reversed relative to each other. Takaishi et al. synthesized pyrene or perylene compounds with bulky functional groups at both ends and demonstrated, using their CPL spectra and TD-DFT calculations, that the sign of the CPL derived from a pyrene excimer or a pyrene–perylene exciplex is governed by the twist direction between the dye's planar rings [29–31]. Our results suggest that the chirality (*L*- and *D*-configurations) of the pyrenylalanine unit in a peptide governs the twist direction between the pyrenes, based on their method.

The anisotropy factor, which is a measure of CPL performance, is expressed as a Kuhn asymmetry factor, $g_{CPL} = 2 \times (IL - IR)/(IL + IR)$, where *IL* and *IR* are the intensities of the left and right circularly polarized luminescent components, respectively. (L)-**1** and (L)-**2** exhibited anisotropy factors ($|g_{CPL}|$) of -1.9×10^{-4} and -0.9×10^{-2}, respectively, which were too large for luminophore **2**-emitting excimer CPL. This was attributed to the ability of the peptide to flexibly twist its pyrene rings upon photoexcitation, resulting in a chiral spatial configuration that is well suited for emitting intramolecular excimer CPL.

3. Control of Configuration-Dependent CPL Properties in Optically Active DL–Peptide–Pyrene Organoluminescent Materials [32]

The absolute configurations of the peptides in one optically active peptide–pyrene organoluminescent material were identical, as shown in Section 2. In Section 3, optically active peptide–pyrene organoluminescent materials, namely, (L,D)-**3** and (D,L)-**3,** containing pyrenylalanine with different configurations (Figure 5) were synthesized, and their chiroptical properties in $CHCl_3$ solutions were investigated.

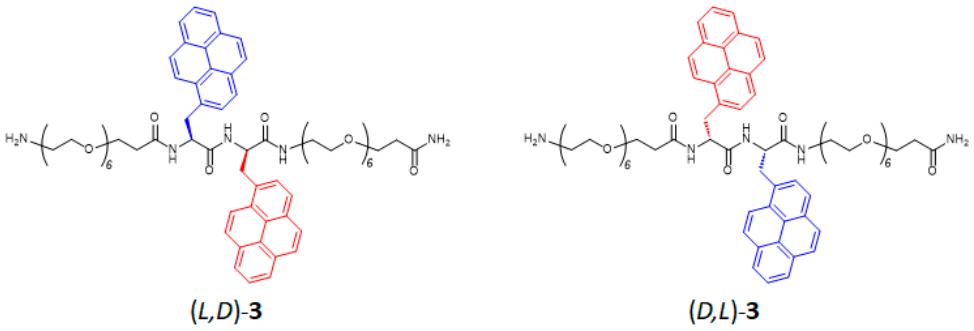

Figure 5. Chemical structures of the chiral peptide–pyrene luminophores (L,D)-**3** and (D,L)-**3**.

First, the CPL properties of (L,D)-**3** and (D,L)-**3** were examined (Figure 6a). Consequently, pyrene excimer-derived CPL with an anisotropy factor of ($|g_{CPL}|$) = 0.5 × 10^{-2} was successfully observed at approximately 450 nm for both (L,D)-**3** and (D,L)-**3**, similar to the case where (L)-**2** exhibited pyrene excimer-derived CPL in Section 2. Interestingly, (L)-**2** exhibited negative (–) CPL, whereas (L,D)-**3** and (D,L)-**3** exhibited negative (–)- and positive (+) CPL, respectively. This indicates that the absolute configuration of the N-terminal amino acid (pyrenylalanine) unit determines the direction of CPL rotation. Furthermore, when amino acid units with different chiralities were introduced into a single molecule, the different chiralities of the amino acid units did not cancel each other out but instead resulted in a synergistic CPL. That is, these results suggest that the mere absolute configuration of the amino acid units in the peptide does not affect the CPL sign, and they indicate that the twist between pyrenes resulting from the absolute configuration of the N-terminal amino acid unit affects the CPL sign.

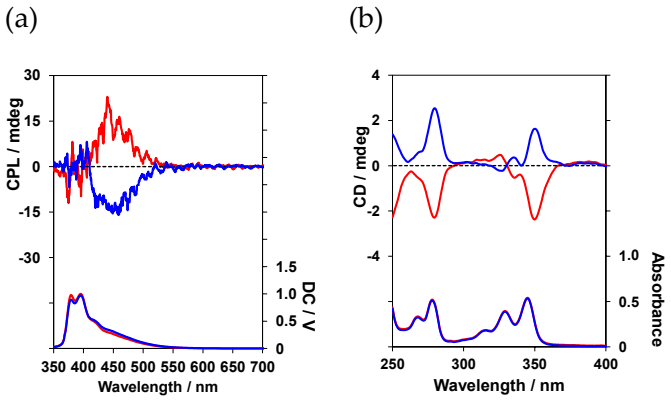

Figure 6. (**a**) CPL (top) and PL (bottom) spectra, and (**b**) CD (top) and absorption (bottom) spectra of (L,D)-**3** (blue lines) and (D,L)-**3** (red lines) in $CHCl_3$ solutions.

Next, CD spectra were acquired to investigate the chiral environment of the luminescent pyrene unit in its ground state (Figure 6b). The CD spectra of an equimolecular mixture of two absolute configurations, such as L-pyrenylalanine and D-pyrenylalanine, are usually expected to show no Cotton effect owing to the nullification of the different chiralities. However, both (L,D)-**3** and (D,L)-**3** exhibited clear CD profiles. (L)-**2** exhibited

a positive (+)-CD Cotton effect, whereas (L,D)-**3** and (D,L)-**3** exhibited positive (+)- and negative (–)-CD Cotton effects, respectively, at the longest absorption wavelength. This suggests that the absolute configuration of the N-terminal amino acid unit determines the chiral spatial configuration of the pyrene unit, even in the ground state.

In summary, a synergistic CPL effect was successfully created by changing the combination of the absolute configurations of the amino acid units in the peptide backbone.

4. Control of the Pyrene Number-Dependent CPL Properties in Optically Active Peptide–Pyrene Organoluminescent Materials [33]

The effect of the number of pyrene rings located within a peptide on the chiroptical properties of optically active peptide–pyrene luminescent materials was investigated. Peptide–pyrene luminescent materials (L)-**4** to (L)-**6** and (D)-**4** to (D)-**6** were synthesized with fixed distances between the pyrenylalanine units and different numbers of pyrene rings in the peptides: two, four, and six (Figure 7). In these peptide–pyrene luminescent materials, glycine units were used as alkyl spacers.

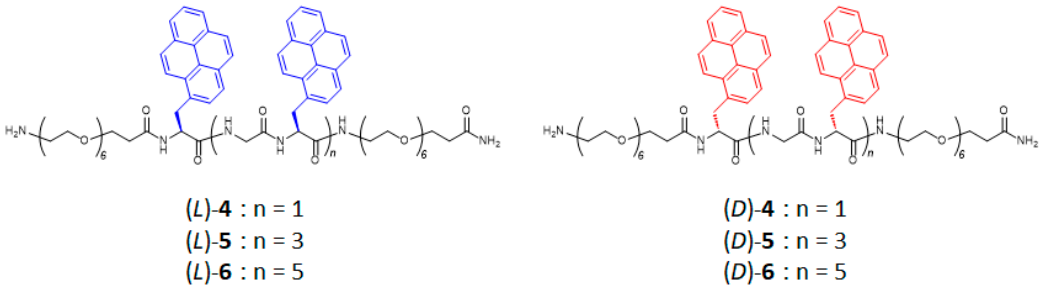

Figure 7. Chemical structures of the chiral peptide–pyrene luminophores (L)-**4** to (L)-**6** and (D)-**4** to (D)-**6**.

CPL spectra of (L)-**4**, (L)-**5** and (L)-**6** in $CHCl_3$ solution with different numbers of pyrene rings are shown in Figure 8a–c; for (L)-**4**, both monomeric and excimer CPL from pyrene units was observed. However, for (L)-**5** and (L)-**6**, CPL properties were not observed. (L)-**5** and (L)-**6** were too low in solubility in a $CHCl_3$ solution compared with (L)-**4**, and aggregates were likely formed when they were mixed with $CHCl_3$. Indeed, the $CHCl_3$ solution was a turbid suspension that did not properly transmit light. Therefore, CPL could not be detected. (L)-**1**, with one pyrene unit, emitted weak monomeric CPL at a maximum luminescence wavelength (λ_{em}) of approximately 398 nm and a maximum luminescence wavelength (λ_{em}) of approximately 482 nm. The signs of the CPL spectra between (L)-**4** and (D)-4 were reversed relative to each other. (L)-**4** exhibited an anisotropy factor ($|g_{CPL}|$) of -2.0×10^{-3} for excimer CPL.

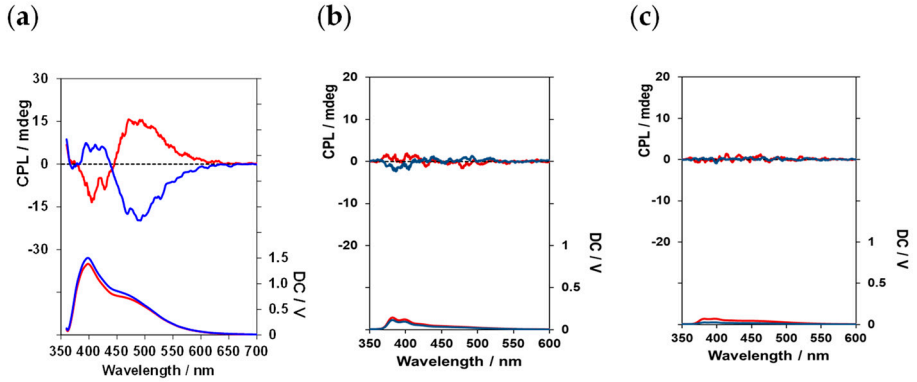

Figure 8. CPL (top) and PL (bottom) spectra of (**a**) (L)-**4** (blue lines) and (D)-**4** (red lines), (**b**) (L)-**5** (blue lines) and (D)-**5** (red lines), and (**c**) (L)-**6** (blue lines) and (D)-**6** (red lines) in $CHCl_3$ solutions.

To investigate the ground-state chirality of (L)-**4**, (L)-**5** and (L)-**6**, we compared CD and UV-vis absorption spectra in $CHCl_3$ solution (Figure 9a–c). Clear UV-vis absorption spectra and the corresponding CD spectra were observed for (L)-**4**; however, although the UV-vis absorption spectra were very weak owing to the aggregation of the peptide–pyrene luminophores, the signals of the CD spectra for (L)-**5** and (L)-**6** were observed.

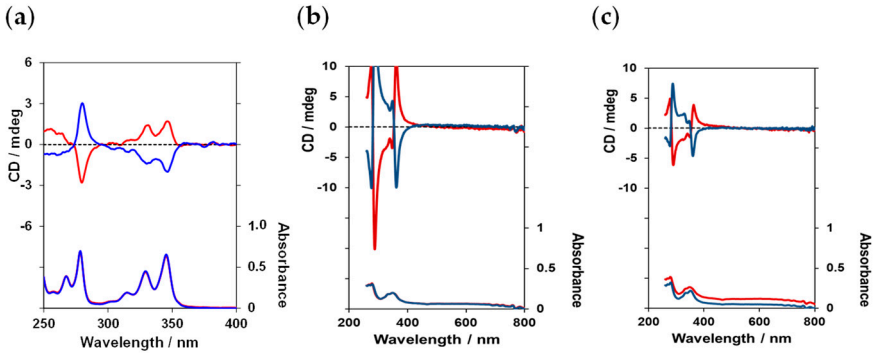

Figure 9. CD (top) and absorption (bottom) spectra of (**a**) (L)-**4** (blue lines) and (D)-**4** (red lines), (**b**) (L)-**5** (blue lines) and (D)-**5** (red lines), and(**c**) (L)-**6** (blue lines) and (D)-**6** (red lines) in $CHCl_3$ solutions.

When the solvent was changed from the $CHCl_3$ solution to a methanol solution, the CD and CPL properties were similar in both solutions.

The results of these CD and CPL properties indicate that it is likely that aggregates are formed between pyrene units when the number of pyrene units increases in Gly peptides. Therefore, in the following experiments, we investigated the optical properties of a peptidopyrene luminescent material with two pyrene rings.

5. Control of Distance-Dependent CPL Properties in Optically Active Peptide–Pyrene Organoluminescent Materials [34]

The distance between the two pyrene rings located within the peptide and its effects on the chiroptical properties of the optically active peptide–pyrene luminescent materials were investigated. For this purpose, (L)-**7** to (L)-**14** and (D)-**7** to (D)-**14**, in which alkyl spacers with different chain lengths were introduced between the two pyrenylalanine units in the peptide, were synthesized (Figure 10). Eight types of alkyl spacers were used, from glycine units (n = 1) and β-alanine units (n = 2) to 9-aminononanoic acid units (n = 8), with the number of carbon atoms increasing by one. These units were expected to change the distance between pyrenylalanines by approximately 1.5 Å for each additional C–C bond, and to change their orientation between pyrene rings according to the even-odd rule.

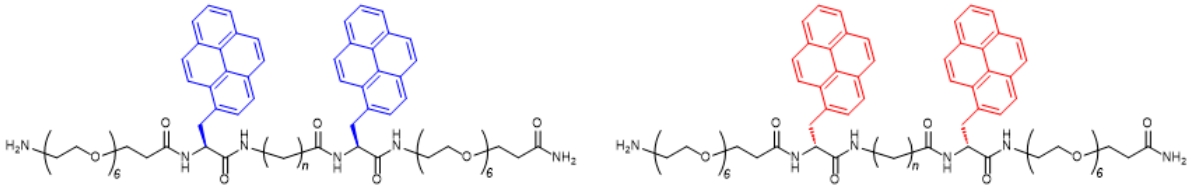

(*L*)-**7** : n = 1 (*L*)-**11** : n = 5
(*L*)-**8** : n = 2 (*L*)-**12** : n = 6
(*L*)-**9** : n = 3 (*L*)-**13** : n = 7
(*L*)-**10** : n = 4 (*L*)-**14** : n = 8

(*D*)-**7** : n = 1 (*D*)-**11** : n = 5
(*D*)-**8** : n = 2 (*D*)-**12** : n = 6
(*D*)-**9** : n = 3 (*D*)-**13** : n = 7
(*D*)-**10** : n = 4 (*D*)-**14** : n = 8

Figure 10. Chemical structures of the chiral peptide–pyrene luminophores (L)-**7** to (L)-**14**, and (D)-**7** to (D)-**14**.

First, their CD spectra were determined in $CHCl_3$ solutions to investigate the chiral environment of the luminescent pyrene units in the ground state of the 16 optically active peptide–pyrene luminophores (Figure 11).

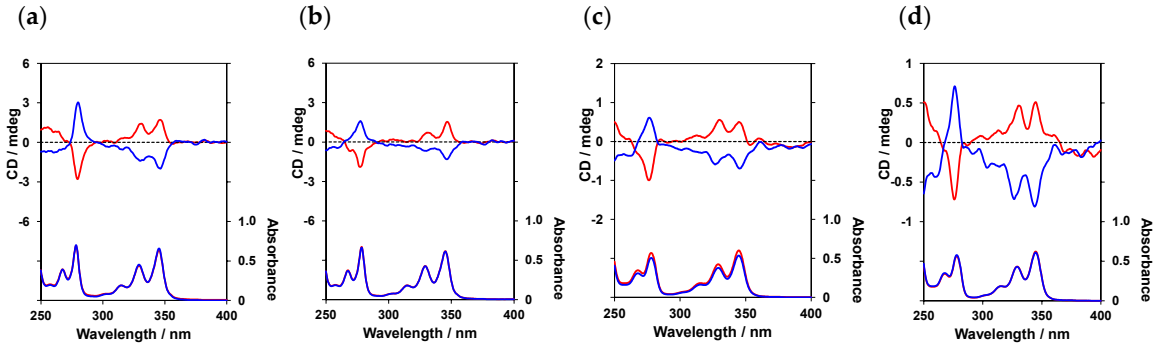

Figure 11. CD (top) and absorption (bottom) spectra of (**a**) (L)-**7** (blue lines) and (D)-**7** (red lines), (**b**) (L)-**8** (blue lines) and (D)-**8** (red lines), (**c**) (L)-**12** (blue lines) and (D)-**12** (red lines), and (**d**) (L)-**13** (blue lines) and (D)-**13** (red lines) in $CHCl_3$ solutions.

The CD and absorption spectra were similar, regardless of the number of carbons in the peptide main chain between the pyrenes, with the Cotton effect observed at approximately 346 nm at the longest wavelength. The same signs of the CD spectra of the (L) and (D) peptide–pyrene luminophores suggests that the relative chiral arrangements of the two intramolecular pyrene rings of the peptides, which had the same absolute configuration, were all the same in the ground state.

The PL and CPL spectra of **7**–**14** (Figure 12) were then measured. The PL spectra exhibited an increase in excimer-derived fluorescence near 500 nm as the alkyl spacer length was increased. Evaluations of the fluorescence spectra at various peptide concentrations revealed that such excimer formation occurs within peptides rather than between peptides [35]. This result suggests that the forced proximity to the two pyrene rings through the alkyl spacer in the peptide prompts their excimer formation. Furthermore, this result indicates that the alkyl spacers are sufficiently flexible to not interfere with the proximity of the two pyrenes.

Interestingly, when the number of carbons between the pyrenes in the peptide main chain increased from one (in **7**) to two (in **8**), CPL inversion occurred in the CPL spectra (Figure 12a,b). The intensity of monomeric luminescence decreased, whereas excimer luminescence increased, as described above, with an increasing number of carbons between the pyrenes in **7**–**10**. Additionally, the anisotropy factor ($|g_{CPL}|$) became stronger, in the order of 10^{-2}, resulting in strong CPL. CPL sign reversal occurred again as the number of carbons in the peptide main chain between the pyrenes increased from six (in **12**) to seven (in **13**) (Figure 9c,d).

Notably, the CD spectra signs were the same in luminophores (L)-**7** to (L)-**14** and (D)-**7** to (D)-**14** with the same absolute configuration, whereas only the CPL spectrum exhibited a sign reversal. This indicates that the relative chiral configurations of the intramolecular pyrene rings are the same in optically active peptide–pyrene luminescent materials with the same absolute configuration in the ground state; however, the relative configuration between the changes in the intramolecular pyrene with the inter-pyrene distance was only observed in the photoexcited state. Therefore, this result indicates that the distance between the alkyl spacers between the pyrenes influences the excimer formation of the two pyrene rings and their twisting. The expected even–odd rule provided by the alkyl groups was not reflected in the CPL results. The pyrenes in these peptides show that the distance and orientation provided by the alkyl spacers between them act in a complex way to influence the sign and strength of the CPL.

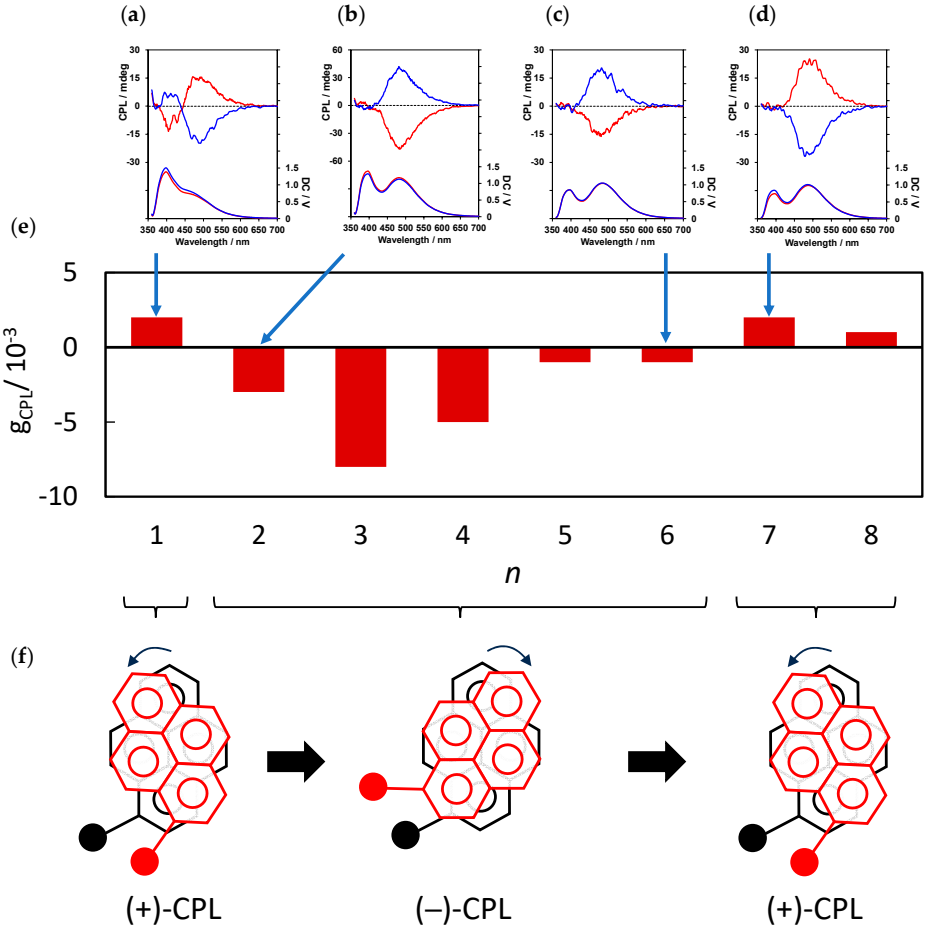

Figure 12. CPL (top) and PL (bottom) spectra of (**a**) (L)-**7** (blue lines) and (D)-**7** (red lines), (**b**) (L)-**8** (blue lines) and (D)-**8** (red lines), (**c**) (L)-**12** (blue lines) and (D)-**12** (red lines), and (**d**) (L)-**13** (blue lines) and (D)-**13** (red lines) in $CHCl_3$ solutions. (**e**) g_{CPL} values as a function of the number of alkyl spacers (*n* in Figure 10) in (D)-**7** to (D)-**14**. (**f**) A plausible schematic illustration of the twist between two pyrenes in the peptides. The two pyrenyl groups in the peptide are expected to twist in a counterclockwise or clockwise manner, depending on the number of alkyl spacers, thus changing the CPL sign.

In summary, the direction of CPL rotation in optically active peptide–pyrene luminescent materials was successfully controlled by changing the distance between the luminescent pyrenes and varying the chirality of the peptide main chains.

6. Control of Solvent-Dependent CPL Properties in Optically Active Peptide–Pyrene Organoluminescent Materials [36,37]

Sections 2–5 described the control of CPL properties via changing the molecular design of optically active peptide–pyrene organoluminescent materials. This section focusses on optically active peptide–pyrene luminophores (**10**), in which the number of carbons between the two pyrenes was four (n = 4) and investigates the solvent-dependent CPL properties of these peptides (Figure 13). Four solvents, namely $CHCl_3$, dichloromethane (CH_2Cl_2), *N*,*N*-dimethylformamide (DMF), and methanol (MeOH), were used for the CPL measurements.

Figure 14a,b shows the CPL spectra of (L)-**10** and (D)-**10** in $CHCl_3$ and CH_2Cl_2, respectively. Both samples exhibited excimer CPL due to intramolecular pyrene interactions, with maximum CPL wavelengths (λ_{CPL}) of 484 and 478 nm, respectively, and anisotropy factors, $|g_{CPL}|$, of 0.5×10^{-2} for both. The CPL properties were also examined in polar DMF and MeOH (Figure 14c,d). Notably, (L)-**10** exhibited a positive (+) CPL in $CHCl_3$ and CH_2Cl_2,

whereas it exhibited a negative (–) CPL in DMF and MeOH. The λ_{CPL} values were 464 and 458 nm, and the anisotropy factors, $|g_{CPL}|$, were 0.2×10^{-2} and 0.3×10^{-2}, in DMF and MeOH, respectively. These results indicate that changes in the environment around peptides, which differ between non-polar solvents (CH_2Cl_2 and CH_3Cl) and polar solvents (DMF and MeOH), affect CPL properties. That is, the difference in solvent polarity affects the structural flexibility of the peptide chain and the interaction between the solvent and functional groups, such as the amide and pyrenyl groups within the peptide, resulting in these changes prompting a change in the twist between the two pyrene units.

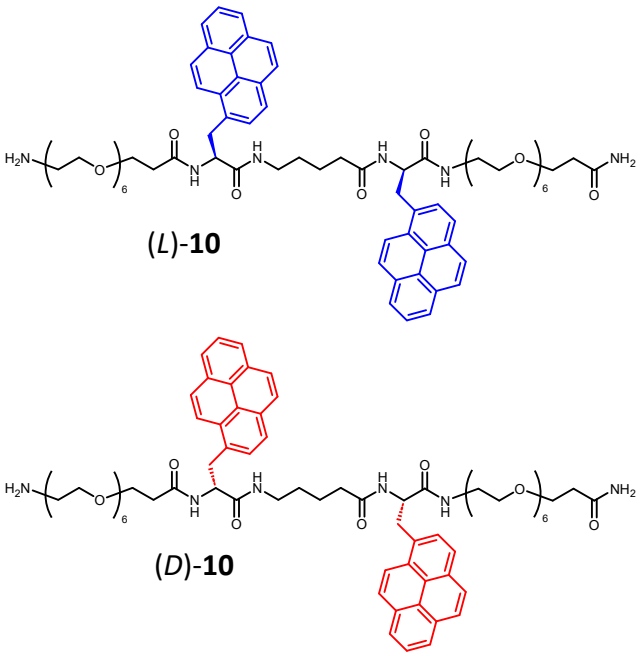

Figure 13. Chemical structures of the chiral peptide–pyrene luminophores (L)-**10** and (D)-**10**.

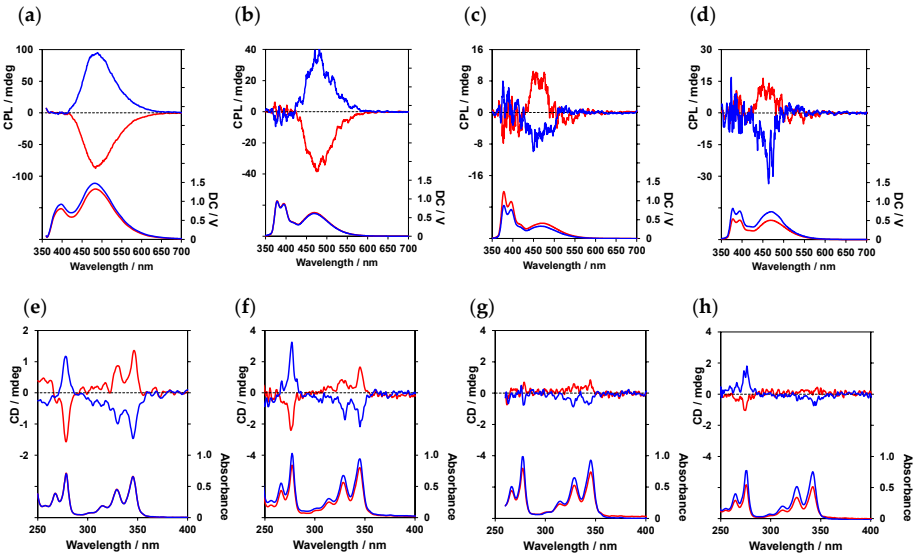

Figure 14. CPL (top) and PL (bottom) spectra of (L)-**10** and (D)-**10** in (**a**) $CHCl_3$, (**b**) CH_2Cl_2, (**c**) DMF, and (**d**) MeOH solutions, and CD (top) and absorption (bottom) spectra of (L)-**10** and (D)-**10** in (**e**) $CHCl_3$, (**f**) CH_2Cl_2, (**g**) DMF, and (**h**) MeOH solutions.

CD spectra were also acquired to investigate the chiral environment of the luminescent pyrene units in the ground state (Figure 14e–h). The sign of the Cotton effect at the longest

wavelength (345–346 nm) was the same in all solvents, being negative (–) for (L)-**10** and positive (+) for (D)-**10**, suggesting that an inversion of chirality in different solvents occurs only in the photoexcited state.

In summary, the direction of CPL rotation in optically active peptide–pyrene luminescent materials was successfully controlled by changing the type of solvent used in addition to the chirality of the peptide main chain.

Subsequently, peptide–pyrene–piperidine organoluminescent materials, (L)-**15** and (D)-**15**, as shown in Figure 15, were synthesized. These peptides consisted of (L)-**10** and (D)-**10** backbones containing piperidine units on both sides of the peptides, and their solvent-dependent CPL-controlled on–off switching properties were investigated.

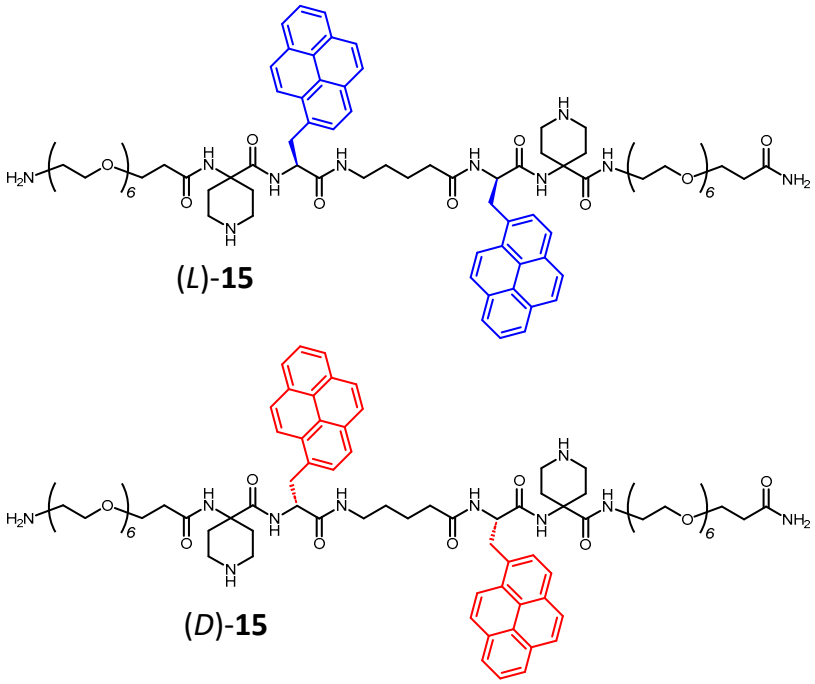

Figure 15. Chemical structures of the chiral peptide–pyrene-piperidine luminophores (L)-**15** and (D)-**15**.

Similar to the CPL spectra measurements, the CD spectra were acquired using the same four solvents, namely $CHCl_3$, CH_2Cl_2, DMF, and MeOH. When peptide–pyrene luminescent (L)-**10** was used, positive (+) CPL was observed in the $CHCl_3$ and CH_2Cl_2 solutions, and negative (–) CPL was observed in the DMF and MeOH solutions. However, when piperidine-incorporated luminescent (L)-**15** was used, all exhibited positive (+) CPLs (Figure 16a–d). This suggests that the introduction of piperidine units on both sides of the peptide main chain suppressed the inversion of the solvent-dependent CPL. This may have been due to the steric effect that the piperidine rings impart to the peptide and the interaction between the two piperidine rings and the solvent. The anisotropy factors ($|g_{CPL}|$) in the $CHCl_3$, CH_2Cl_2, DMF, and MeOH solutions were 0.4×10^{-2} (λ_{CPL} = 470 nm), 0.4×10^{-2} (λ_{CPL} = 455 nm), 0.4×10^{-2} (λ_{CPL} = 485 nm), and 0.3×10^{-2} (λ_{CPL} = 495 nm), respectively. The CD spectra of (L)-**15** and (D)-**15** were also acquired (Figure 16e–h). Similar to (L)-**10** and (D)-**10**, the Cotton effect at the longest wavelength (341–347 nm) was negative (–) and positive (+) for (L)-**15** and (D)-**15**, respectively, in all solvents.

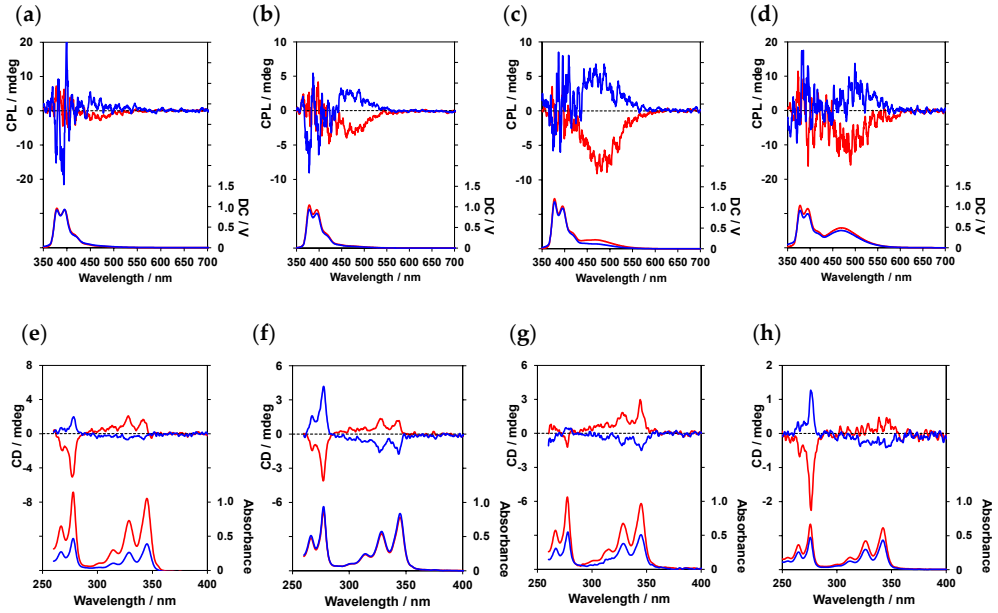

Figure 16. CPL (top) and PL (bottom) spectra of (L)-**15** and (D)-**15** in (**a**) $CHCl_3$, (**b**) CH_2Cl_2, (**c**) DMF, and (**d**) MeOH solutions. CD (top) and absorption (bottom) spectra of (L)-**15** and (D)-**15** in (**e**) $CHCl_3$, (**f**) CH_2Cl_2, (**g**) DMF, and (**h**) MeOH solutions.

The solvent-dependent CPL properties on optically active peptide–pyrene organoluminescent materials in the presence or absence of piperidine units in the peptide backbone was successfully controlled.

7. Conclusions

This study investigated non-classical CPL properties by controlling the pyrene rings as luminescent units incorporated in the main chain of peptides. Control was achieved using (1) the absolute configuration of the pyrenylalanine units (Sections 2 and 3), (2) the number of pyrene units introduced in the peptides (Section 4), (3) the distance of the pyrenylalanine units using an alkyl spacer introduced in the peptides (Section 5), and (4) the solvent (Section 6). In particular, in (3), both left- and right-rotating CPLs were produced using optically active peptide–pyrene organoluminescent materials with the same absolute configuration.

CPL research is in its early stages, and it is anticipated that CPL will be applied in various fields, including circularly polarized white light sources, circularly polarized lasers, CPL sensors, CPL FETs, plant growth control using CPL, absolute asymmetric synthesis using CPL, and the elucidation of the origin of asymmetry in life. The authors expect that this study will help expand the design of new circularly polarized luminescent materials.

Author Contributions: Conceptualization, Y.I. and M.K.; writing—original draft, Y.I.; visualization, Y.I. and M.K.; funding acquisition, Y.I.; writing—review and editing, M.K. All authors have read and agreed to the published version of the manuscript.

Funding: Part of this research was supported by the Japan Society for the Promotion of Science (JSPS) KAKENHI, grant numbers 21K18940 and 21K05030.

Institutional Review Board Statement: Not applicable.

Informed Consent Statement: Not applicable.

Data Availability Statement: Data presented in this study are available on request from the corresponding author.

Acknowledgments: We express our deepest gratitude to Motohiro Shizuma at the Osaka Research Institute of Industrial Science and Technology for his advice on NMR and mass spectrometry.

Conflicts of Interest: The funders had no role in the design of the study; in the collection, analyses, or interpretation of data; in the writing of the manuscript; in the decision to publish the results.

References

1. Dai, Y.; Chen, J.; Zhao, C.; Feng, L.; Qu, X. Biomolecule-Based Circularly Polarized Luminescent Materials: Construction, Progress, and Applications. *Angew. Chem. Int. Ed.* **2022**, *61*, e202211822. [CrossRef]
2. Sisido, M.; Egusa, S.; Okamoto, A.; Imanishi, Y. Circularly Polarized Fluorescence of Aromatic Poly (α-Amino Acids). *J. Am. Chem. Soc.* **1983**, *105*, 3351–3352. [CrossRef]
3. Egusa, S.; Sisido, M.; Imanishi, Y. One-dimensional Aromatic Crystals in Solution. 4. Ground- and Excited-State Interactions of Poly(L-1-Pyrenylalanine) Studied by Chiroptical Spectroscopy Including Circularly Polarized Fluorescence and Fluorescence-Detected Circular Dichroism. *Macromolecules* **1985**, *18*, 882–889. [CrossRef]
4. Sisido, M. One-dimensional Aromatic Crystals in Solution. 9. Synthesis, Conformation, and Chiroptical Spectroscopy of Poly[Lys(Z)2-PyrAla] in Solution. *Macromolecules* **1989**, *22*, 3280–3285. [CrossRef]
5. Inai, Y.; Sisido, M.; Imanishi, Y. Strong Circular Polarization in the Excimer Emission from a Pair of Pyrenyl Groups Linked to a Polypeptide Chain. *J. Phys. Chem.* **1990**, *94*, 2734–2735. [CrossRef]
6. Sasaki, H.; Sisido, M.; Imanishi, Y. Switching of Excimer/Monomer Ratio in Chiral Bilayer Membranes Containing Pyrenyl Groups. *Langmuir* **1990**, *6*, 1008–1012. [CrossRef]
7. Li, C.; Jin, X.; Zhao, T.; Zhou, J.; Duan, P. Optically Active Quantum Dots with Induced Circularly Polarized Luminescence in Amphiphilic Peptide Dendron Hydrogel. *Nanoscale Adv.* **2019**, *1*, 508–512. [CrossRef] [PubMed]
8. Krupová, M.; Kapitán, J.; Bouř, P. Induced Lanthanide Circularly Polarized Luminescence as a Probe of Protein Fibrils. *ACS Omega* **2019**, *4*, 1265–1271. [CrossRef] [PubMed]
9. Jiang, P.; Liu, W.; Li, Y.; Li, B.; Yang, Y. pH-influenced Handedness Inversion of Circularly Polarized Luminescence. *New J. Chem.* **2021**, *45*, 21941–21946. [CrossRef]
10. Li, Q.; Zhang, J.; Wang, Y.; Zhan, G.; Qi, W.; You, S.; Su, R.; He, Z. Self-Assembly of Peptide Hierarchical Helical Arrays with Sequence-Encoded Circularly Polarized Luminescence. *Nano Lett.* **2021**, *21*, 6406–6415. [CrossRef] [PubMed]
11. Li, M.; Liu, M.; Sha, Y. Induced and Inversed Circularly Polarized Luminescence of Achiral Thioflavin T Assembled on Peptide Fibril. *Small* **2022**, *18*, 2106130–2106137. [CrossRef]
12. Wang, X.; Zhao, L.; Wang, C.; Feng, X.; Ma, Q.; Yang, G.; Wang, T.; Yan, X.; Jiang, J. Phthalocyanine-Triggered Helical Dipeptide Nanotubes with Intense Circularly Polarized Luminescence. *Small* **2022**, *18*, 2104438–2104446. [CrossRef]
13. Lian, T.; Liu, W.; Li, Y.; Yang, Y. Molecular Packing Structural Transition Driven Handedness Inversion of Circularly Polarized Luminescence of Phenothiazine Substituted Phe–Phe Dipeptides. *New J. Chem.* **2023**, *47*, 653–659. [CrossRef]
14. Wang, Z.; Hao, A.; Xing, P. Halogen Interaction Effects on Chiral Self-Assemblies on Cyclodipeptide Scaffolds Across Hierarchy. *Small* **2023**, *19*, 2302517–2302527. [CrossRef] [PubMed]
15. Zhang, Y.; Sun, Y.; Li, G.; Du, M.; Sheng, N.; Shen, J. Fluorescent Hydrogels with Emission Enhancement and CPL-activity Depending on Gelation States. *J. Mater. Chem. C* **2023**, *11*, 3292–3299. [CrossRef]
16. Wang, W.; Wang, Z.; Sun, D.; Li, S.; Deng, Q.; Xin, X. Supramolecular Self-Assembly of Atomically Precise Silver Nanoclusters with Chiral Peptide for Temperature Sensing and Detection of Arginine. *Nanomaterials* **2022**, *12*, 424–437. [CrossRef] [PubMed]
17. Xin, X.; Gao, Y.; Zhang, Q.; Wang, Z.; Sun, D.; Yuan, S.; Xia, H. Realizing Enhanced Luminescence of Silver Nanocluster–Peptide Soft Hydrogels by PEI Reinforcement. *Soft Matter* **2018**, *14*, 8352–8360. [CrossRef] [PubMed]
18. Cheng, L.; Tian, P.; Duan, H.; Li, Q.; Song, X.; Li, A.; Cao, L. Chiral Adaptive Recognition with Sequence Specificity of Aromatic Dipeptides in Aqueous Solution by an Achiral Cage. *Chem. Sci.* **2023**, *14*, 833–842. [CrossRef]
19. Yan, C.; Li, Q.; Miao, X.; Zhao, Y.; Li, Y.; Wang, P.; Wang, K.; Duan, H.; Zhang, L.; Cao, L. Chiral Adaptive Induction of an Achiral Cucurbit [8]uril-Based Supramolecular Organic Framework by Dipeptides in Water. *Angew. Chem. Int. Ed.* **2023**, *135*, e202308029. [CrossRef]
20. Wang, Z.; Ai, H.; Hao, A.; Xing, P. Biomimetic Chiral Molecular Tweezers Based on Tryptophan-Containing Peptides with Chiroptical Evolution. *Chem. Mater.* **2022**, *34*, 10162–10171. [CrossRef]
21. Neil, E.R.; Fox, M.A.; Pal, R.; Parker, D. Induced Europium CPL for the Selective Signalling of Phosphorylated Amino-Acids and O-Phosphorylated Hexapeptides. *Dalton Trans.* **2016**, *45*, 8355–8366. [CrossRef] [PubMed]
22. Shi, Y.; Yin, G.; Yan, Z.; Sang, P.; Wang, M.; Brzozowski, R.; Eswara, P.; Wojtas, L.; Zheng, Y.; Li, X.; et al. Helical Sulfono-γ-AApeptides with Aggregation-Induced Emission and Circularly Polarized Luminescence. *J. Am. Chem. Soc.* **2019**, *141*, 12697–12706. [CrossRef]
23. Brichtová, E.; Hudecová, J.; Vršková, N.; Šebestík, J.; Bouř, P.; Wu, T. Binding of Lanthanide Complexes to Histidine-Containing Peptides Probed by Raman Optical Activity Spectroscopy. *Chem. Eur. J.* **2018**, *24*, 8664–8669. [CrossRef]
24. Zhang, Y.; Yang, D.; Han, J.; Zhou, J.; Jin, Q.; Liu, M.; Duan, P. Circularly Polarized Luminescence from a Pyrene-Cyclodextrin Supra-Dendron. *Langmuir* **2018**, *34*, 5821–5830. [CrossRef] [PubMed]
25. Nishikawa, T.; Tajima, N.; Kitamatsu, M.; Fujiki, M.; Imai, Y. Circularly Polarised Luminescence and Circular Dichroism of L- and D-Oligopeptides with Multiple Pyrenes. *Org. Biomol. Chem.* **2015**, *13*, 11426–11431. [CrossRef]

26. Kitamatsu, M.; Nakamura-Tachibana, A.; Ishikawa, Y.; Michiue, H. Improvement of Water Solubility of Mercaptoundecahydrododecaborate (BSH)-Peptides by Conjugating with Ethylene Glycol Linker and Interaction with Cyclodextrin. *Processes* **2021**, *9*, 167–177. [CrossRef]
27. Shigeto, H.; Kishi, T.; Ishii, K.; Ohtsuki, T.; Yamamura, S.; Kitamatsu, M. Adjusting the Structure of a Peptide Nucleic Acid (PNA) Molecular Beacon and Promoting its DNA Detection by a Hybrid with Quencher-Modified DNA. *Processes* **2022**, *10*, 722–732. [CrossRef]
28. Kitamatsu, M.; Inoue, K.; Yamagata, N.; Michiue, H. Reaction of Chloroacetyl-Modified Peptides with Mercaptoundecahydrododecaborate (BSH) Is Accelerated by Basic Amino Acid Residues in the Peptide. *Processes* **2022**, *10*, 2200–2208. [CrossRef]
29. Takaishi, K.; Iwachido, K.; Ema, T. Solvent-Induced Sign Inversion of Circularly Polarized Luminescence: Control of Excimer Chirality by Hydrogen Bonding. *J. Am. Chem. Soc.* **2020**, *142*, 1774–1779. [CrossRef]
30. Takaishi, K.; Murakami, S.; Iwachido, K.; Ema, T. Chiral Exciplex Dyes Showing Circularly Polarized Luminescence: Extension of the Excimer Chirality Rule. *Chem. Sci.* **2021**, *12*, 14570–14576. [CrossRef]
31. Takaishi, K.; Maeda, C.; Ema, T. Circularly Polarized Luminescence in Molecular Recognition Systems: Recent Achievements. *Chirality* **2023**, *35*, 92–103. [CrossRef]
32. Mimura, Y.; Nishikawa, T.; Fuchino, R.; Nakai, S.; Tajima, N.; Kitamatsu, M.; Fujiki, M.; Imai, Y. Circularly Polarised Luminescence of Pyrenyl Di- and Tri-Peptides with Mixed D- and L-Amino Acid Residues. *Org. Biomol. Chem.* **2017**, *15*, 4548–4553. [CrossRef]
33. Mimura, Y.; Motomura, Y.; Kitamatsu, M.; Imai, Y. Development of Circularly Polarized Luminescence (CPL) Peptides Containing Pyrenylalanines and 2-Aminoisobutyric Acid. *Processes* **2020**, *8*, 1550–1557. [CrossRef]
34. Nishikawa, T.; Kitamura, S.; Kitamatsu, M.; Fujiki, M.; Imai, Y. Peptide Magic: Interdistance-Sensitive Sign Inversion of Excimer Circularly Polarized Luminescence in Bipyrenyl Oligopeptides. *ChemistrySelect* **2016**, *4*, 831–835. [CrossRef]
35. Mimura, Y.; Motomura, Y.; Kitamatsu, M.; Imai, Y. Controlling the Sign of Excimer-Origin Circularly Polarised Luminescence by Balancing Hydrophilicity/Hydrophobicity in Bipyrenyl Arginine Peptides. *Asian J. Org. Chem.* **2021**, *10*, 149–153. [CrossRef]
36. Mimura, Y.; Kitamura, S.; Shizuma, M.; Kitamatsu, M.; Fujiki, M.; Imai, Y. Solvent-sensitive Sign Inversion of Excimer-origin Circularly Polarized Luminescence in Bipyrenyl Peptides. *ChemistrySelect* **2017**, *2*, 7759–7764. [CrossRef]
37. Mimura, Y.; Kitamura, S.; Shizuma, M.; Kitamatsu, M.; Imai, Y. Circular Dichroism and Circularly Polarised Luminescence of Bipyrenyl Oligopeptides, with Piperidines added in the Peptide Chains. *Org. Biomol. Chem.* **2018**, *16*, 6895–6901. [CrossRef]